Complex Molecular Mechanism for Dihydropyridine Binding to L-Type Ca2+Channels As Revealed by Fluorescence Resonance Energy Transfer

ARTICLE *in* BIOCHEMISTRY · OCTOBER 1994

Impact Factor: 3.02 · DOI: 10.1021/bi00205a025

6 AUTHORS, INCLUDING:

Jörg Striessnig
University of Innsbruck
222 PUBLICATIONS **10,785** CITATIONS
SEE PROFILE

Richard Paul Haugland
Starfish Country Home School
144 PUBLICATIONS **13,081** CITATIONS
SEE PROFILE

Complex Molecular Mechanism for Dihydropyridine Binding to L-Type Ca^{2+}-Channels As Revealed by Fluorescence Resonance Energy Transfer†

Wolfgang Berger, Heino Prinz,‡ Jörg Striessnig, Hee-Chol Kang,§ Richard Haugland,§ and Hartmut Glossmann*

Institut für Biochemische Pharmakologie, University of Innsbruck, Peter Mayr-Strasse 1, A-6020 Innsbruck, Austria

Received June 3, 1994; Revised Manuscript Received July 21, 1994®

ABSTRACT: We analyzed binding-induced changes in the fluorescence properties of the 1,4-dihydropyridine (DHP), DMBODIPY-DHP [(−)-1,4-dihydro-2,6-dimethyl-4-(2-trifluoromethylphenyl)-3,5-pyridinedicarboxylic acid 2-[4,4-difluoro-5,7-dimethyl-4-bora-3a,4a-diaza-3-(s-indacene)propionylamino]ethylethyl ester)], to study the molecular mechanisms underlying the interaction of DHPs with the α_1-subunit of skeletal muscle L-type Ca^{2+} channels. The quantum yield of the fluorophore DMBODIPY was similar in solvents of different polarity. In contrast, the quantum yield of DMBODIPY-DHP was low in buffer but increased with solvent polarity and upon specific binding. This indicates the existence of binding-induced changes of intramolecular quenching of the fluorophore by the DHP moiety. Specific ligand binding also induced fluorescence resonance energy transfer (FRET) between one or more tryptophanes of the channel protein and the DMBODIPY-DHP fluorophore. The specific FRET signal was successfully used to directly measure DHP binding at high time resolution. It revealed complex association and dissociation kinetics of DMBODIPY-DHP although no site heterogeneity was detected in equilibrium experiments. We therefore fitted our data to a binding scheme considering one or more intermediate conformational states for the formation of the ligand–receptor complex. Such a step-wise binding mechanism explains previously observed differences in the binding site densities and the kinetic constants determined for different DHPs using conventional binding (for example filtration) assays.

Depolarization-induced Ca^{2+} influx into electrically excitable cells is mediated through different types of voltage-dependent Ca^{2+} channels (Bean, 1989). L-Type Ca^{2+} channels are expressed in the plasma membrane of neuronal, muscle, and endocrine cells. They are sensitive to different chemical classes of drugs, such as dihydropyridines (DHPs)[1] (for example, nifedipine and isradipine), phenylalkylamines (for example, verapamil and devapamil), and benzothiazepines [for example, (+)-*cis*-diltiazem] (Glossmann & Striessnig, 1990). These drugs stereoselectively bind with nanomolar dissociation constants to distinct binding domains on the channel that appear allosterically coupled (Glossmann & Striessnig, 1990). The domains are located on the α_1-subunit of the channel complex as revealed by photoaffinity labeling with domain-selective probes. Regions that form the DHP and phenylalkylamine binding domains were recently identified within the primary structure of the α_1-subunit (Catterall & Striessnig, 1992). The availability of several high affinity ligands for the different binding domains together with our increasing knowledge about L-type Ca^{2+}-channel structure make α_1-subunits highly suitable to study the molecular basis of drug–ion channel interactions and of drug binding to macromolecules in general (Prinz & Striessnig, 1993).

Radiolabeled DHPs became the preferred biochemical tools for the sensitive detection of low concentrations of L-type Ca^{2+} channels in excitable cells. A comparison of the binding properties of different radiolabeled DHPs led to the conclusion that a complex molecular mechanism must underlie DHP Ca^{2+} channel interaction (Glossmann et al., 1985). First, considerable differences exist for the kinetics of DHP binding, distinguishing DHPs with rapid and slow binding kinetics, respectively. The diastereomers of the DHP Ca^{2+} antagonist [^{35}S]sadopine are a particularly interesting example. Despite identical affinity of the two diastereoisomers, their rate constants differ about 10-fold (Knaus et al., 1992b). Secondly, significant differences in the maximal number of binding sites were described for various radiolabeled DHPs [for a review, see Glossmann et al. (1985)]. This could neither be explained by the differential labeling of channel-unrelated DHP binding sites nor by differences in their dissociation constants (Glossmann et al., 1985). Instead, it has been proposed that DHPs differ with respect to their ability to stabilize a high affinity binding state (Glossmann et al., 1985). So far no attempts have been made to explain these observations in terms of a molecular binding mechanism.

In order to get detailed insight into the molecular mechanisms of DHP–Ca^{2+} channel interaction, we decided to study DHP binding at high time resolution. For this purpose we analyzed changes of the fluorescence properties of a fluorescent DHP, DMBODIPY-DHP,[1] that occur upon specific binding of the drug to its domain on the α_1-subunit. We find that specific binding increases the fluorescence yield of DMBODIPY-DHP and allows fluorescence resonance energy transfer (FRET) to occur between the ligand and one or more tryptophan residues of the α_1-subunit. This enables the direct

†This work was supported by grants from the Fonds zur Förderung der Wissenschaftlichen Forschung (S6601 to H.G. and S6602 to J.S.), the Bundesministerium für Wissenschaft und Forschung (to H.G.), and the Dr. Legerlotz Foundation (to J.S.).

* To whom correspondence should be addressed.

‡ Max-Planck Institut für Molekulare Physiologie, Rheinlanddamm 201, D-44139 Dortmund, Germany.

§ Molecular Probes Inc., 4849 Pitchford Ave., Eugene, OR 97402.

® Abstract published in *Advance ACS Abstracts,* September 1, 1994.

[1] Abbreviations: B_{max}, maximal density of binding sites; DHP, 1,4-dihydropyridine; DMBODIPY-PAc, (4,4,-difluoro-5,7-dimethyl-4-bora-3a,4a-diaza)-3-(s-indacene)propionic acid; DMBODIPY-DHP, (−)-1,4-dihydro-2, 6-dimethyl-4-(2-trifluoromethylphenyl)-3,5-pyridinedicarboxylic acid 2-[4,4-difluoro-5,7-dimethyl-4-bora-3a,4a-diaza-3-(s-indacene)propionylamino]ethylethyl ester; DMSO, dimethyl sulfoxide; FRET, fluorescence resonance energy transfer; K_d, dissociation constant; IC_{50}, EC_{50} concentration causing 50% binding inhibition or stimulation, respectively; n_H, slope factor; PMSF, phenylmethanesulfonyl fluoride.

0006-2960/94/0433-11875$04.50/0

quantification of α_1-subunit-bound drug at high time resolution without separation of bound and free ligand. Using this technique, we measured complex binding kinetics for DMBODIPY-DHP. On the basis of a quantitative analysis, we propose a molecular mechanism of step-wise reversible DHP binding to L-type Ca^{2+} channels. Such a step-wise binding mechanism explains previously observed differences in binding site densities determined for different DHPs using conventional binding (e.g., filtration) assays.

MATERIALS AND METHODS

Materials. DMBODIPY-DHP was synthesized as previously described (Knaus et al., 1992b). (+)-[^{3}H]Isradipine (75 Ci/mmol) and [^{3}H]BAYK8644 (80 Ci/mmol) were from NEN (Vienna, Austria). The unlabeled enantiomers of various phenylalkylamines and of isradipine were kindly provided by Dr. Traut (Knoll AG, Ludwigshafen, Germany) and Sandoz AG (Basel, Switzerland), respectively. Digitonin was from Biosynth AG (Staad, Switzerland). Protease inhibitors and other chemicals were from Sigma (Deisenhofen, Germany). Wheat germ agglutinin Sepharose 4B was synthesized as described (Striessnig & Glossmann, 1991).

Ca^{2+} Channel Purification. For fluorescence binding studies Ca^{2+} channels were partially purified from rabbit skeletal muscle after solubilization in 1% (w/v) digitonin by affinity chromatography on wheat germ agglutinin–Sepharose 4B according to previously published procedures (Striessnig & Glossmann, 1991). The glycoprotein fraction contained about 150 pmol/mg of protein of Ca^{2+} channel associated DHP binding sites as determined by conventional (+)-[^{3}H]-isradipine binding assays (Glossmann & Ferry, 1985). Protein concentrations were determined using the Bradford assay (Bradford, 1976).

Fluorescence Binding Studies (Charcoal Assay). Binding studies with DMBODIPY-DHP were carried out at 25 °C in binding buffer [50 mM Tris–HCl, pH 7.6, 0.1% (w/v) digitonin, 0.25 mg/mL bovine serum albumin (essentially fatty acid free), 0.1 mM $CaCl_2$] in a final volume of 1 mL as previously described (Knaus et al., 1992a). Fluorescent and nonfluorescent drugs were diluted in dimethyl sulfoxide (DMSO) and directly added to the incubation mixture. The final DMSO concentration did not exceed 1% (v/v), which did not affect ligand binding. To separate bound and free DMBODIPY-DHP, the samples were cooled on ice (2 min) and then rapidly mixed with 0.25 mL of an ice-cold charcoal suspension (40 mg/mL in distilled water). After incubation for 10 min on ice the charcoal was removed by centrifugation. 0.075 mL of 1.5% (w/v) digitonin was added to the supernatant, and the fluorescence was measured in a Perkin-Elmer LS50B spectrofluorimeter (excitation at 488 nm, slit width, 4 nm; emission at 517 nm, slit width, 10 nm) in quartz cuvettes. Cuvettes were siliconized before use to minimize the adsorption of drugs and protein. Nonspecific binding was determined in the presence of 1.5 μM (+)-isradipine. The concentration of added fluorescent ligand was calculated from standard curves prepared for DMBODIPY-DHP in binding buffer.

Fluorescence Resonance Energy Transfer (FRET) Assays. FRET assays were carried out under incubation conditions identical to those described for charcoal assays. For equilibrium experiments assays were incubated in Eppendorf tubes. Samples were then transferred into quartz cuvettes, and FRET was measured at 517 nm (1.5–10 nm slit width depending on the signal amplitude) with excitation at 285 nm (4 nm slit width). To measure association kinetics, DMBODIPY-DHP in binding buffer was added to a temperature-controlled quartz cuvette. The association reaction was started by addition of partially purified Ca^{2+}-channel protein (0.05–0.2 mL, 1 mL final incubation volume) under constant stirring. Dissociation reactions were induced by the addition of the indicated concentrations of the nonfluorescent competitive inhibitor (+)-isradipine. In kinetic experiments the data sampling rate was between 3 and 60 data points per minute. In control experiments no photobleaching of DMBODIPY-DHP or tryptophan was detectable after 3 h of continuous excitation at 285 or 488 nm under the above experimental conditions. Most nonfluorescent Ca^{2+} antagonists, including the enantiomers of isradipine, did not affect FRET up to concentrations of 10 μM. At concentrations >3 μM, (+)-*cis*-diltiazem and (+)-tetrandrine decreased FRET fluorescence, most likely due to inner filter effects. A slight increase in background FRET fluorescence was found in the presence of desmethoxyverapamil at concentrations above 3 μM affecting equilibrium binding data by less than 10% at 10 μM. The concentration of specifically bound DMBODIPY-DHP from FRET fluorescence was calculated from standard curves relating FRET fluorescence to specifically bound drug as determined by the charcoal assay. Control FRET experiments revealed that less than 5% of specific equilibrium binding was lost under the conditions of charcoal treatment (10 min, 2 °C).

Calculation of Relative Quantum Yields of DMBODIPY-DHP and Its Fluorescent Moiety DMBODIPY-PAc. From both compounds 1 mM stock solutions were prepared in DMSO. Drugs were further diluted in solvents of different polarity to measure absorption (10 μM) as well as fluorescence excitation and emission spectra (0.1 μM; absorbance at 488 nm < 0.008). Absorption spectra were recorded in a Hitachi U-2000 spectrophotometer. DMBODIPY-DHP was sufficiently soluble at 10 μM concentrations in the selected solvents. Further experimental conditions are given in the legend to Figure 1. Relative quantum yields (Q_{rel}) in different solvents were expressed as the ratio of the area under the fluorescence emission spectra in the respective solvent (F_{solv}) and in 50% (v/v) glycerol ($F_{glycerol}$). Areas were corrected for differences in absorbance at the exciting wavelength (488 nm):

$$Q_{rel} = \frac{F_{solv}}{F_{glycerol}} \times \frac{A_{glycerol}}{A_{solv}}$$

The relative quantum yield of specifically receptor-bound DMBODIPY-DHP was determined by comparing the fluorescence (excitation, 488 nm; emission, 517 nm) per picomole of specifically bound DMBODIPY-DHP with the fluorescence of free DMBODIPY-DHP in the same buffer (buffer A). The fluorescence per picomole of bound DMBODIPY-DHP was calculated from saturation studies with DMBODIPY-DHP (to determine maximally bound fluorescence) and radiolabeled (+)-[^{3}H]isradipine (to determine maximal DHP binding capacity) in parallel and under identical assay conditions (charcoal assay). Maximally bound fluorescence and radioactivity were determined by fitting the binding data to a monophasic binding isotherm.

Data Analysis and Calculations. Equilibrium binding parameters (K_d and B_{max}) were obtained by Scatchard analysis of saturation experiments. Inhibition curves were computer-fitted to the general dose–response equation (DeLean et al., 1978) using nonlinear least-squares curve fitting. Data are given as means ± standard deviation from the indicated number of experiments.

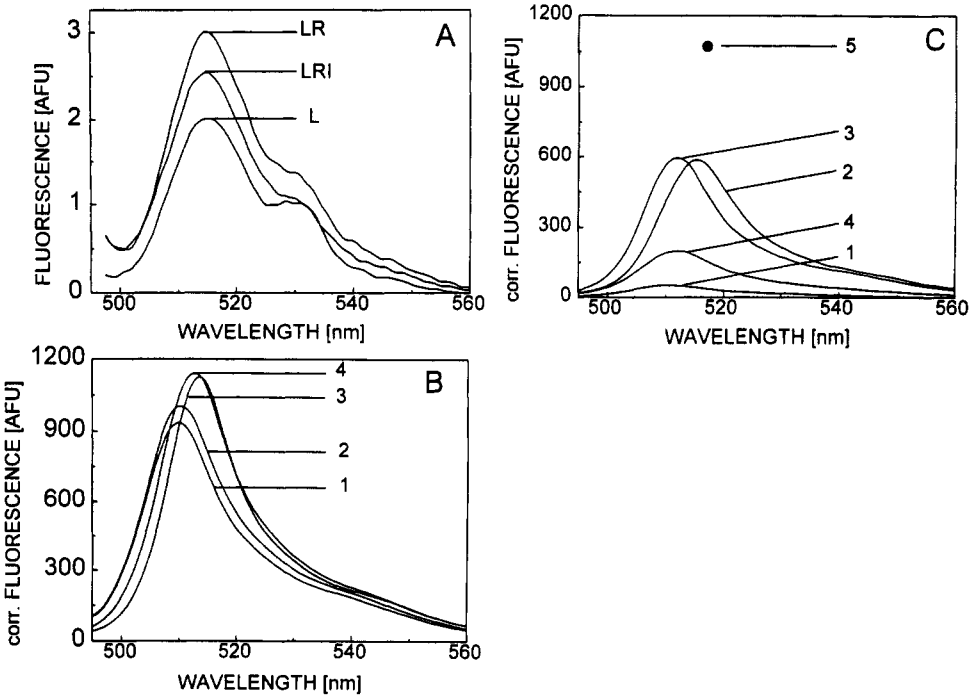

FIGURE 1: Relative quantum yield of DMBODIPY-DHP and DMBODIPY-PAc. Fluorescence emission spectra were recorded at 25 °C (slit width, 1.5 nm) after excitation at 488 nm (slit width, 4 nm). (A) Increase of DMBODIPY-DHP fluorescence upon drug binding. L, ligand (2.2 nM) in 0.8 mL of binding buffer (containing 0.1% digitonin). LR, 0.2 mL of partially purified DHP receptor protein (0.04 mg/mL, 7.8 nM DHP binding sites) was added and the spectrum recorded after binding equilibrium was reached (30 min). LRI, spectrum recorded after dissociation of saturable binding (45 min) with nonfluorescent (+)-isradipine (1.5 μM final concentration). The calculated concentration of LR in equilibrium was 0.81 nM. (B and C) Quantum yield of DMBODIPY in different solvents. Emission spectra of (B) the fluorophore DMBODIPY (employed as DMBODIPY-PAc) and (C) the fluorescent ligand DMBODIPY-DHP were recorded (excitation 488 nm) in 0.1 μM solutions of different solvents: water (1), 0.1% (w/v) digitonin (2), 2-propanol (3), and 50% (v/v) glycerol (4). Spectra were corrected for differences in absorption at 488 nm. Spectra recorded in binding buffer differed less than 10% from the spectrum obtained in 0.1% (v/v) digitonin alone. In separate experiments (see Results) a 1.95-fold higher quantum yield was determined for the receptor-bound DMBODIPY-DHP at 517 nm and is indicated in C (5).

Simultaneous Fits. Details of the simultaneous curve-fitting procedure are given in the legend to Table 2. During prolonged incubation of ligand–receptor complexes under continuous registration of FRET, a slow decay of the specific signal with time was evident. This decay did not vary between different receptor preparations but was clearly temperature-dependent, increasing at higher temperatures. Control experiments revealed that it was not due to ligand-induced "desensitization" of binding activity, because the rate constant of the decay was indistinguishable in the absence or presence of added ligand (not shown). Photobleaching of the fluorophores (tryptophan or DMBODIPY-DHP) at 285 nm excitation could also be excluded (not shown). Because the decay also increased in the absence of added Ca^{2+}, it was most likely due to the irreversible inactivation of binding activity reported in earlier studies (Schneider et al., 1991; Striessnig et al., 1986). This slow time-dependent inactivation was taken into account for the quantitative analysis of our binding data (see below).

Table 1: Relative Quantum Yield of DMBODIPY-DHP and DMBODIPY-PAc in Solvents of Different Polarity[a]

	DMBODIPY-PAc		DMBODIPY-DHP	
solvent	Q	λ_{max}	Q	λ_{max}
50% glycerol in H_2O	1.000	512.5	0.181	512
H_2O	0.834	510	0.046	509
0.1% digitonin in H_2O	0.918	510	0.511	515
acetonitrile	0.859	509	0.229	510
ethanol	0.801	512.5	0.363	511
2-propanol	0.919	513.5	0.503	512
hexane	0.699	510	n.d.	n.d.

[a] Ten micromolar solutions of DMBODIPY-DHP and DMBODIPY-PA were prepared in the respective solvents, and emission spectra were recorded as described in the legend to Figure 1B,C. The areas under the emission curves were calculated by integration and corrected for absorbance at the exciting wavelength (488 nm, see Materials and Methods). Data were normalized for the highest relative quantum yield determined (DMBODIPY-PAc in 50% glycerol). nd, not determined; λ_{max}, emission wavelength maximum. Means of duplicate determinations are shown.

RESULTS

Increase in DMBODIPY-DHP Fluorescence upon Drug Binding. Our goal was to exploit changes in the fluorescence properties of DMBODIPY-DHP upon specific binding that could serve as a signal to directly quantify specifically bound ligand in the presence of free ligand. Figure 1 shows that the relative quantum yield of DMBODIPY-DHP was low in detergent-free buffer but increased 10-fold (Table 1) in the presence of 0.1% (w/v) digitonin. It further increased upon specific binding to the α_1-subunit. Figure 1A illustrates the emission spectra of DMBODIPY-DHP (2.2 nM final concentration) before (L) and after addition (LR) of channel protein. This increase was partially reversed after addition of the nonfluorescent competitor (+)-isradipine (LRI) to 1.5 μM. Under these experimental conditions about half of the increase could be attributed to the specific binding of DMBODIPY-DHP. To obtain a more precise estimate of this fluorescence increase, saturation experiments were carried out in parallel with DMBODIPY-DHP and (+)-[^{3}H]isradipine under identical experimental conditions (see Materials and Methods). By correlating maximally receptor-bound fluorescence (excitation, 488 nm; emission, 517 nm) with the maximal DHP binding capacity as determined by (+)-[^{3}H]-isradipine, we calculated that the fluorescence signal of bound

DMBODIPY-DHP was (1.95 ± 0.4)-fold (n = 4, mean ± SD) higher than of free ligand in assay buffer (containing 0.1% (w/v) digitonin) and about 20-fold higher than in detergent-free buffer (Table 1).

To investigate the underlying mechanism of this binding-induced change in quantum yield, we compared the relative quantum yield of DMBODIPY-DHP (Figure 1C) and of the DMBODIPY fluorophore alone (employed as the propionic acid derivative, DMBODIPY-PAc) (Figure 1B) in buffer and solvents of different polarity. In contrast to the DHP derivative, the quantum yield of DMBODIPY-PAc itself was only weakly dependent on the polarity of the solvent and was not affected by the addition of digitonin to the binding buffer (Figure 1 and Table 1). For DMBODIPY-DHP a much lower quantum yield was observed in polar solvents, that increased with decreasing polarity of the organic solvent as well as in 0.1% digitonin. The quantum yield of specifically bound DMBODIPY-DHP (measured only at 517 nm) was similar to the quantum yield of DMBODIPY-PAc. These results indicate that the DHP moiety causes intramolecular quenching of DMBODIPY in the DMBODIPY-DHP molecule. It must be due to stacking of the substituted DHP ring and the DMBODIPY fluorophore in polar solvents that is disrupted by less polar solvents and upon drug binding. This fluorescence increase could serve as a signal to directly detect specifically bound ligand. However, the signal to noise ratio decreases at low ratios of bound to free ligand due to the increasing background fluorescence of free ligand. We therefore sought for an alternative approach to directly quantify specifically bound DMBODIPY-DHP.

Direct Measurement of DMBODIPY-DHP Binding Using FRET. Figure 2A illustrates the emission spectrum of the partially purified DHP receptor preparation after excitation at 285 nm. Protein fluorescence occurs between 300 and 400 nm, with a maximum at 336 nm. At this excitation wavelength this is mostly due to the fluorescence of tryptophan residues (Lakowicz, 1983). The emission maximum was below the maximum found for free tryptophan in aqueous solutions (348 nm). A similar blue-shift of tryptophan emission has been previously reported for other proteins (for example human serum albumin) (Lakowicz, 1983). The emission spectrum of the Ca^{2+} channel (DHP receptor) preparation overlapped over the whole range with a portion of the excitation spectrum of DMBODIPY-DHP. Therefore FRET should theoretically be possible between the two fluorophores provided that they are within the critical distance (usually ≈ 2–5 nm; Lakowicz, 1983; Stryer & Haugland, 1967) required for effective transfer. We tested this possibility by measuring the emission of DMBODIPY-DHP after excitation at 285 nm before and after addition of receptor protein. The respective emission spectra of DMBODIPY-DHP between 500 and 550 nm are illustrated in Figure 2B. Background fluorescence was observed for receptor protein (R) in binding buffer (buffer A). Weak fluorescence was measured for DMBODIPY-DHP alone exhibiting minimal excitation at wavelengths below 300 nm (Figure 2A). Addition of receptor protein to ligand-containing buffer resulted in a time-dependent increase of DMBODIPY-DHP fluorescence within a time range characteristic for the formation of the DMBODIPY-DHP–channel complex (Knaus et al., 1992c) (see below). Dissociation of the complex by addition of a saturating concentration of the nonfluorescent competitor (+)-isradipine reversed this signal. This indicates that the fluorescence increase above background was due to saturable high affinity drug binding. No FRET signal was induced by the addition of bovine serum albumin

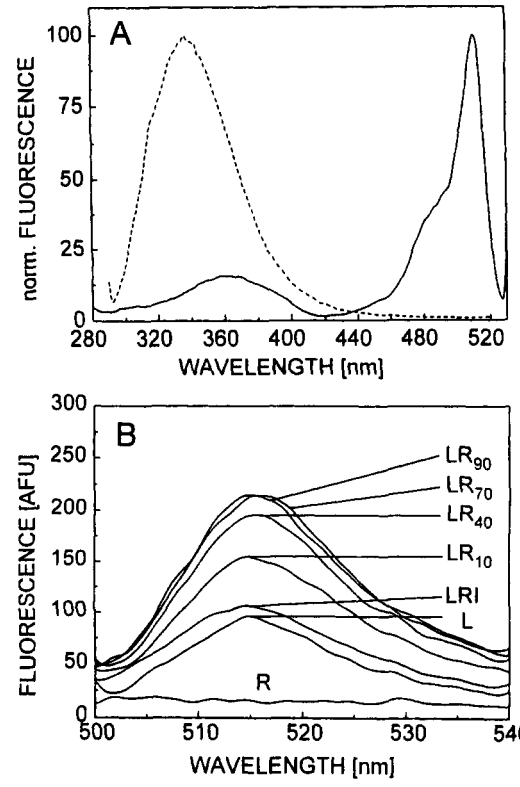

FIGURE 2: Fluorescence resonance energy transfer between Ca^{2+} channel tryptophan residues and DMBODIPY-DHP. (A) Spectral overlap of protein emission spectrum and DMBODIPY-DHP excitation spectrum. (- - -) Emission spectrum of 0.018 mg/mL of partially purified receptor preparation in binding buffer, excitation was at 285 nm. (—) Excitation spectrum of DMBODIPY-DHP (36 nM). Arbitrary fluorescence units were normalized with respect to the highest data points. norm, normalized. (B) Emission spectra of DMBODIPY-DHP in the absence and presence of receptor protein after excitation at 285 nm. R, receptor (1.9 nM) alone in buffer A; L, ligand (32.5 nM) before addition of receptor protein; LR10, LR40, LR70, and LR90, recordings 10, 40, 70, and 90 min after addition of receptor protein. LRI, recording after dissociation of saturable DMBODIPY-DHP binding by 1.5 μM (+)-isradipine (90 min). Incubation temperature for all spectra was 9 °C to slow association and dissociation kinetics (association half-life, >10 min). LR_{10}, LR40, LR70, and LR90 spectra were not corrected for time-dependent changes in complex concentration during recording. The calculated concentration of specifically bound DMBODIPY-DHP was 1.4 nM.

alone (1 mg/mL, not shown) or when DMBODIPY-PAc, which lacks high affinity for DHP receptors, was incubated with channel protein under identical experimental conditions (not shown).

To demonstrate that FRET can be used to directly quantify the concentration of formed complex in the presence of free ligand, we related the saturable FRET signal (excitation 285 nm) to the concentration of specifically bound DMBODIPY-DHP (excitation 488 nm) determined in parallel using the conventional charcoal assay. FRET linearly correlated over a wide range of receptor (1.5–8.8 nM) and ligand concentrations (2.3–163 nM) with DMBODIPY-DHP binding (not shown). This was also evident from saturation experiments (Figure 3A). The difference in the binding parameters (filled circles, FRET; open circles, charcoal assay) were within the experimental error. An excellent correlation was also found when the concentration of specifically bound DMBODIPY-DHP was modulated by other Ca^{2+}-channel drugs (illustrated in Figure 3B for inhibition by the isradipine enantiomers). FRET fluorescence was stereoselectively modulated with the pharmacological profile expected for DMBODIPY-DHP binding to L-type Ca^{2+} channels (Knaus et al., 1992c).

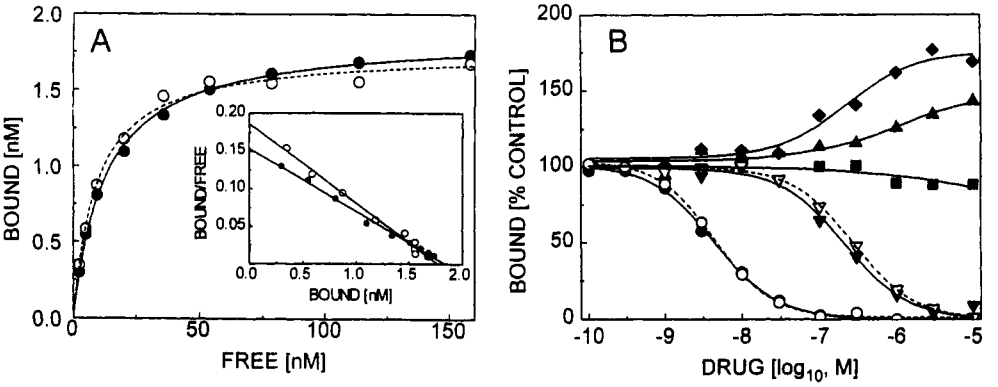

FIGURE 3: Equilibrium binding properties and pharmacological profile of DMBODIPY-DHP binding to L-type Ca^{2+} channels using FRET. (A) Saturation anlysis: 0.018 mg/mL partially purified DHP receptor protein was incubated for 60 min with increasing concentrations of DMBODIPY-DHP in the absence (total binding) or presence (nonspecific binding) of 1.5 μM (+)-isradipine (1 mL final assay volume). Total ligand concentration was measured by excitation at 488 nm. First, specific FRET fluorescence was obtained by excitation of the samples at 285 nm (emission measured at 517 nm). The concentration of specifically bound DMBODIPY-DHP was determined in the same samples using the charcoal assay (open circles). For each ligand concentration FRET fluorescence was plotted against the concentration of bound ligand as shown in Figure 2C. The factor (1 nM complex = 124 FRET fluorescence units, $n = 9$, $r = 0.98$) relating the two signals was calculated by linear regression analysis and used to convert FRET fluorescence into bound DMBODIPY-DHP concentration (filled circles). Data points are means ± SD from triplicate determinations. The binding parameters (drawn lines) obtained were as follows: charcoal assay, K_d = 9.3 nM, B_{max} = 1.8 nM (100 pmol/mg of protein); FRET, K_d = 12.8 nM, B_{max} = 1.9 nM. (Inset) Scatchard transformation. (B) Modulation of DMBODIPY-DHP binding as determined by FRET. DMBODIPY-DHP (8.6–10.1 nM) was incubated with partially purified DHP receptor in the absence (control) or presence of nonfluorescent Ca^{2+} antagonists. Binding in the presence of drugs is expressed as percent of control binding. The following binding parameters were obtained: (●) (+)-isradipine, IC_{50} = 4.4 nM (K_i = 2.5 nM), n_H = 1.08; (▼) (−)-isradipine, IC_{50} = 208 (K_i = 117 nM), n_H = 1.07; (▲) (+)-*cis*-diltiazem, EC_{50} = 1.05 μM, n_H = 0.70 (assuming maximum stimulation to 150%); (■) (−)-*cis*-diltiazem: $IC_{50} \gg 10$ μM; (◆), (+)-tetrandrine, IC_{50} = 219 nM, n_H = 0.96. One of three similar experiments is shown. To illustrate the correlation of the FRET signal with the concentration of bound DMBODIPY-DHP, inhibition by the isradipine enantiomers was measured by charcoal assay in parallel (open symbols). (○) (+)-isradipine, IC_{50} = 4.4 nM (K_i = 2.5 nM), n_H = 1.19; (▽) (−)-isradipine, IC_{50} = 272 nM (K_i = 153 nM), n_H = 1.11.

The simplicity of the FRET technique makes it especially useful for kinetic studies. Association and dissociation kinetics of DMBODIPY-DHP measured using FRET are illustrated in Figure 4. As expected, they occurred with time constants similar to those previously measured using the charcoal assay. In contrast to charcoal assays, whose limited accuracy and time resolution suggested monophasic reactions (Knaus et al., 1992c), FRET revealed more complex kinetic components. Both dissociation and association reactions performed with a 10-fold excess of ligand (i.e., pseudo-first-order conditions) showed a curved semilogarithmic plot (see inserts in Figure 4B). Moreover, these experiments were described significantly better by two-exponential reactions than by single exponentials ($p < 0.0001$, F-test). The dissociation rate of DMBODIPY-DHP slightly increased as a function of (+)-isradipine concentration used to induce dissociation (Figure 4C). Dilution-induced dissociation could also be measured using FRET. Preformed complexes were diluted 20-fold into binding buffer in the cuvette, and the FRET signal was recorded immediately. In contrast to the dissociation of (+)-*cis*-diltiazem (Prinz & Striessnig, 1993), dilution-induced dissociation to a new steady-state equilibrium occurred clearly faster than ligand-induced dissociation. This finding was reproducibly obtained in three independent experiments.

As expected for DHPs, drugs interacting with the benzothiazepine binding domain, (+)-*cis*-diltiazem (Figure 4C) and (+)-tetrandrine (not shown), slowed DMBODIPY-DHP binding kinetics in a concentration-dependent manner. Semilogarithmic plots of dissociation reactions remained curved in the presence of (+)-*cis*-diltiazem (Figure 4C).

Development of a Simple Model for DHP Binding. We analyzed our experiments in terms of the simplest possible reaction scheme that quantitatively describes our data. The reaction scheme must be compatible with the existence of multiple kinetic components despite the lack of evidence for more than one DHP binding domain in equilibrium experiments (saturation analysis and binding inhibition studies, Figure 3A). This can be rationalized by a step-wise binding mechanism, where one binding site is occupied in conjunction with conformational changes of the receptor–ligand complex (scheme A):

$$L + R \rightleftharpoons LR' \rightleftharpoons LR'' \rightleftharpoons \ldots \rightleftharpoons LR$$

where L is the ligand (DMBODIPY-DHP) and R is the receptor (DHP binding domain) and LR′ and LR″ indicate intermediate drug–receptor complexes during the formation of the high affinity complex LR. On the structural level binding scheme A can be simply explained by conformational rearrangements of the ligand–receptor complex, proceeding from one or more initial low affinity complexes to a high affinity complex.

We calculated our data with one (scheme A1 in Figure 5) as well as two (scheme A2 in Figure 5) intermediates. One intermediate complex (LR′) was sufficient to describe our data within the experimental error (Figure 4A). As expected for a more complex model, the addition of a second intermediate (LR″) increased the quality of the fits (Figure 4B, see below). Scheme B in Figure 5 is the simplest reaction describing (+)-isradipine binding (added in dissociation kinetic experiments to prevent DMBODIPY-DHP association). It was sufficient to fit our data (see below). Finally, the slow irreversible inactivation of the receptor is accounted for in scheme C (Figure 5), where XR denotes L-type Ca^{2+} channels that have lost binding activity (see Materials and Methods).

Curve Fitting. Simultaneous fits of eleven sets of experiments (see Materials and Methods) using schemes A1 or A2, B, and C resulted in the rate constants shown in Table 2. The fitting strategy was as follows: To measure the slow irreversible loss of binding activity (expressed as k_x), the slow part of the association reaction as monitored over the time range of 8 h was fitted to scheme C. The resulting value for k_x (Table 2) was used for all subsequent fits. Then all association reactions

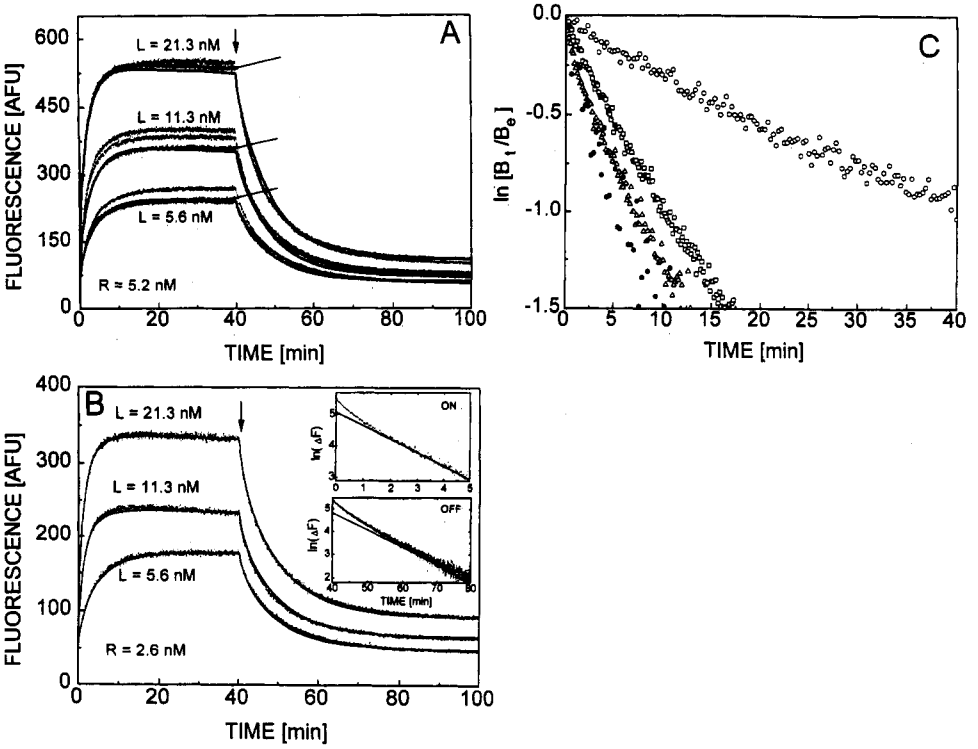

FIGURE 4: Analysis of DMBODIPY-DHP binding kinetics using FRET: quantitative analysis in terms of a simple binding model.. All experiments were performed at 25 °C. Excitation was at 285 nm; emission was recorded at 517 nm. Raw data, not corrected for background fluorescence, are shown. The background fluorescence corresponds to the fluorescence measured after complete dissociation of the complex (100 min). In total a set of 11 different experiments (as described in the text) were simultaneously fitted. The respective kinetic constants are given in Table 2. (A) Curve fitting to scheme 1a: Association and dissociation kinetics at different ligand (L) and receptor concentrations (R = 5.2 nM, 0.04 mg/mL of protein). Dissociation was induced after 40 min (vertical arrow) by addition of 5 μL of nonfluorescent (+)-isradipine (1.5 μM final concentration). To illustrate interassay variability, the data of three (L = 21.3 nM), four (L = 11.3 nM), and three experiments (L = 5.6 nM) are shown. The solid curves represent the theoretical curves calculated from the best fits to binding scheme 1a (one conformational intermediate; see Figure 5) for one representative experiment (indicated by long arrows). The fitted values for L were 19.4 nM (theoretical: 21.3 nM), 9.5 nM (theoretical: 11.3 nM) and 6.6 nM (theoretical: 5.6 nM). The fitted value for R was 4.5 nM (theoretical: 5.2 nM). (B) Curve fitting to scheme 1b: The same ligand concentrations as in panel A were used but lower receptor concentration (R = 2.6 nM; 0.02 mg/mL of protein). Curves were fitted to binding scheme 1b (two conformational intermediates; see Figure 5). The explanation for this variability are variations of the concentrations of ligand and receptor. The fitted values for L were 5.16 nM (theoretical: 5.6 nM), 22.05 (11.3 nM), and 25.56 (theoretical: 21.3 nM). The fitted values for R were between 1.72 and 2.88 nM (theoretical: 2.6 nM). (Inset) Semilogarithmic plots of the association (ON, min 0–5) and dissociation (OFF, min 40–80) time course of one of the traces (R = 2.6 nM, L = 21.3 nM). Straight lines were drawn by eye to illustrate the complex binding kinetics. (C) Semilogarithmic plots of dissociation data are shown. (○) Effect of (+)-*cis*-diltiazem on dissociation kinetics. DMBODIPY-DHP (6.9 nM) was incubated with 0.013 mg/mL DHP binding sites in the presence of 10 μM (+)-*cis*-diltiazem. Dissociation was induced by the addition of a final concentration of 1.5 μM (+)-isradipine after equilibrium was reached. (●, □, △) DMBODIPY-DHP dissociation induced by different concentrations of (+)-isradipine and by dilution. DMBODIPY-DHP (16 nM) was incubated at 25 °C with 0.02 mg/mL of partially purified DHP receptor. After equilibrium was reached, aliquots of the incubation mixture were transferred into different quartz cuvettes, and FRET was measured continuously in both samples (7 data points/min). Dissociation was induced by adding a final concentration of 50 nM (□) or 1.5 μM (△) (+)-isradipine. Both data sets were included in the simultaneous fitting procedure. Background fluorescence was defined as fluorescence measured 90 min after inducing dissociation. To determine dilution-induced dissociation (●), 70 nM DMBODIPY-DHP was incubated with 30 nM DHP receptors and incubated for 30 min. The assay mixture (0.05 mL) was then diluted 20-fold into binding buffer in a cuvette. The FRET signal was immediately measured until a new binding equilibrium was reached. One of three experiments yielding almost identical results is shown.

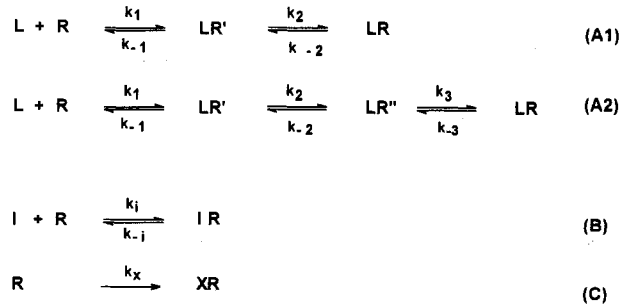

FIGURE 5: Binding schemes used for quantitative analysis. (I) Unlabeled DHP [(+)-isradipine]; (XR) irreversibly inactivated DHP binding site.

were fitted simultaneously in the time range of 0–40 min. This resulted in good estimates for the equilibrium dissociation constants and association rate constants of scheme 1a and 1b. Note that mathematically association and dissociation rate constants are correlated (Prinz & Striessnig, 1993), so that only the equilibrium dissociation constant and the association rate constants were fitted (error given in Table 2). In subsequent fits the dissociation reactions were included, and the rate constants $K_D I$ and k_i of the inhibitor (+)-isradipine were calculated together with all other rate constants. Although intraassay variation was small in our FRET experiments, interassay variability was present, which could in part be attributed to the variable but limited adsorption of drug and receptor protein to the quartz cuvettes. To account for this variability, the concentrations of receptor and ligand had to be used as additional parameters (see the legend to Figure 4A,B). From the parameters fitted to scheme A1 (one intermediate complex) we calculated that the low affinity state LR contributes to 20% ($K_D 2$ = 0.2) of total specific binding, i.e., 80% of the initial binding reactions proceeded to the high affinity state. The apparent affinity of DMBO-

Table 2: Rate Constants and Dissociation Constants Obtained from Simultaneous Curve Fitting[a]

constant	scheme A1	scheme A2
K_{D1}	41 (38–44) nM	125 (103–153) nM
k_1	0.026 (0.025–0.028) nM^{-1} min^{-1}	0.1 (0.08–0.12) nM^{-1} min^{-1}
k_{-1}	1.0 min^{-1}	12.5 min^{-1}
K_{D2} (k_{-2}/k_2)	0.2 (0.18–0.22)	0.16 (0.13–0.20)
k_2	1.3 (1.1–1.5) min^{-1}	1.8 (1.5–2.2) min^{-1}
k_{-2}	0.26 min^{-1}	0.29 min^{-1}
K_{D3} (k_{-3}/k_3)		1.0 (0.96–1.04)
k_3		0.29 min^{-1}
k_{-3}		0.29
K_{D_i}	0.96 (0.78–1.2) nM	0.96 (0.78–1.2) nM
k_i	0.027 (0.023–0.032) nM^{-1} min^{-1}	0.027 (0.023–0.032) nM^{-1} min^{-1}
k_{-i}	0.026 min^{-1}	0.026 min^{-1}
k_x	0.003 min^{-1}	0.003 min^{-1}

[a] The binding mechanism was calculated with the differential equations corresponding to Figure 5 (available on request as FACSIMILE files) by means of the program FACSIMILE (AEA technology, England). The theoretical curves were fitted simultaneously to three different types of experiments: (1) One association reaction (15.6 nM DMBODIPY-DHP, 2.6 nM DHP binding sites) monitored over an extended period of time (8 h) to determine irreversible inactivation of binding activity (see below). (2) Six association reactions initiated by adding 5.6, 11.3, and 21.3 nM DMBODIPY-DHP to 2.6 or 5.2 nM DHP binding sites (panels A and B). (3) Six dissociation reactions initiated by the addition of 1.5 μM (+)-isradipine after equilibrium was reached (i.e., 40 min after the start of incubation) (panels A and B). (4) Four dissociation reactions induced at equilibrium conditions (16 nM DMBODIPY-DHP was incubated with 2.6 nM DHP binding sites for >50 min) initiated by addition of 50 nM (panel C), 150 nM, 500, or 1500 nM (panel C) (+)-isradipine. All experiments were performed at least in triplicate. Individual experiments, representing a set of identical experiments, were used for the simultaneous fitting procedure. To account for interassay variations (Figure 4A), the concentrations of both DMBODIPY-DHP and DHP binding sites were varied within the fitting process. For rate constants, see Figure 5. 5–95% confidence limits are given in parentheses. The rate constants for (+)-isradipine were the same, independent on the binding scheme used to calculate DMBODIPY-DHP binding. Note, that the reactions k_2 and k_3 are first-order reactions (dimension "min^{-1}").

DIPY-DHP for LR was calculated as K_D1K_D2 = 8.4 nM. This quantitative analysis implies that a reaction scheme like scheme 1a is sufficient to describe DMBODIPY-DHP binding within our experimental error.

The velocity of the dissociation reaction was slightly affected by the concentration of (+)-isradipine (Figure 4C) used to induce dissociation. As evident from Table 2, this can be explained by the relatively slow association rate constant (k_i) for (+)-isradipine, which becomes the rate-limiting step of the DMBODIPY-DHP dissociation reaction. This is in agreement with our finding that dissociation induced by rapid dilution was faster than ligand-induced dissociation (Figure 4C). The equilibrium dissociation constant (K_{D_i} = 0.97 nM in Table 2) and the dissociation rate constant (k_{-i} = 0.026 min^{-1}) for (+)-isradipine derived from this simultaneous fits correspond to those previously determined with radiolabeled (+)-[^{3}H]isradipine in partially purified Ca^{2+}-channel preparations (K_D = 1–2 nM, k_{-1} = 0.03 min^{-}, (Knaus et al., 1992c; Striessnig & Glossmann, 1991).

Introduction of a second intermediate (LR″) in particular improved the fit of the association reactions. The fits of the dissociation reactions were also improved, but a small but systematic discrepancy remained: our theoretical curves slightly underestimated the slowly dissociating component (Figure 4B). This could be explained for example by separate pathways for ligand association and dissociation. In general, such a discrepancy reflects the simplicity of scheme A used to describe the complex process of molecular rearrangements.

Variations in the Maximal Number of Partially Purified DHP Binding Domains Detected with Different DHPs. Any step-wise binding mechanism such as described in scheme A cannot directly be detected in equilibrium binding experiments. Under equilibrium conditions, the ratio of the different complexes LR′, LR″, ..., LR is the same at all ligand concentrations. If, however, the dissociation from one or more of the initial complexes is faster than the time required for the separation of bound and free ligand (for example, the filtration time), then they will not be detected in conventional (i.e., dilution–filtration) assays. This will result in a decrease of the apparent B_{max}. Without requiring further structural assumptions, a step-wise mechanism would therefore easily explain why different DHPs were found to label different densities of high affinity sites despite their mutual competitive interaction. In skeletal muscle membranes [^{3}H]BAYK8644 labels only about 10–20% of the sites detected with (+)-[^{3}H]-isradipine (Glossmann et al., 1985). We found a similar difference in our purified Ca^{2+} channel preparation, where [^{3}H]BAYK8644 recognized only 8% of the sites labeled with (+)-[^{3}H]isradipine in satruation studies ([^{3}H]BAYK8644, K_D = 26.6 ± 11 nM, B_{max} = 12.9 ± 5.8 pmol/mg of protein; (+)-[^{3}H]isradipine, K_D = 1.23 ± 0.4, B_{max} = 158 ± 11 pmol/mg of protein). The results from these equilibrium studies provide independent support for a step-wise mechanism (scheme 1) used for our kinetic analysis.

DISCUSSION

In the current study we present a detailed analysis of changes in the fluorescent properties of DMBODIPY-DHP that occur upon specific binding to the channel DHP binding domain. Three conclusions can be drawn from our data:

(1) Binding of DMBODIPY-DHP involves a conformational change of the drug that must be associated with a decrease in the mean distance between the fluorophore and the DHP ring. This is evident from the increase in quantum yield upon specific DMBODIPY-DHP binding.

(2) Channel-bound DMBODIPY-DHP participates in FRET with one or more tryptophan residues within the α_1-subunit. The resulting fluorescence signal is linearly correlated over wide range of ligand concentration with specifically bound DMBODIPY-DHP. It therefore provides a useful assay to determine bound ligand without disturbing binding conditions and to monitor on-line binding kinetics at high time resolution.

(3) FRET analysis of DMBODIPY-DHP binding revealed complex kinetics in conjunction with simple equilibrium binding. This can be rationalized by a step-wise binding mechanism leading to a complex of high affinity via a sequence of intermediate states (scheme 1).

Consequences for the Interpretation of Ligand Binding Data. Reaction scheme 1a (Figure 5) represents the simplest possible scheme that explains complex dissociation kinetics of DMBODIPY-DHP despite the absence of site heterogeneity in equilibrium studies. Any extensions of this model would introduce additional parameters that could be varied in the fitting procedure resulting in a better fit of our data. This was the case when an additional intermediate step (LR″) was considered (scheme 1b). Another possibility would be to consider two pre-existing conformational states of the DHP receptor site. This would also be equivalent to an extension of our scheme 1a allowing direct DHP binding to the complex LR. We did not consider such a model because of its higher complexity and the lack of experimental or biochemical evidence for different conformational states in the absence of ligand.

On the structural level, binding scheme 1 can be simply explained by conformational rearrangements of the ligand–receptor complex, proceeding from one or more initial low affinity complexes to a high affinity complex. Previous studies reporting differences in the B_{max} values for various radiolabeled DHPs can also be easily interpreted on the basis of our model. If dissociation from initial low affinity complexes is fast, only ligand bound in higher affinity complexes may be detected using conventional techniques for separation of bound from free ligand. Therefore the measured apparent B_{max} will critically depend on the equilibrium constant(s) determining rearrangements from low to higher affinity complexes (K_D2 in our scheme 1a). Rapidly dissociating components will only be detectable in assays that do not shift the equilibrium, such as our FRET measurements. We calculated (using scheme 1a) that under equilibrium conditions the initial low affinity complex LR′ will still contribute to about 20% of bound DMBODIPY-DHP.

Moreover, a multistep binding mechanism would also easily account for the differences in the binding kinetics observed for radiolabeled DHPs. A well studied example is the diastereomers of the DHP Ca^{2+} antagonist [^{35}S]sadopine (Knaus et al., 1992b). Association and dissociation kinetics were about 10-fold slower for the (−)-diastereomer. In terms of our model, slow binding and unbinding may be due to the existence of one or more slow conformational rearrangements during the formation of a high affinity complex. For the (equipotent) sadopine diastereomers, differences in rearrangement kinetics must originate from the opposite orientation of their bulky C3-substituents.

Our model may also provide a suitable working hypothesis for the explanation of noncompetitive binding phenomena observed between DHPs and drugs binding to other binding domains on the channel. Stimulation of DHP binding (see Figure 3B) and slowing of the overall dissociation kinetics by noncompetitive modulators, like for example (+)-*cis*-diltiazem (Figure 4C) or (−)-desmethoxyverapamil (Glossmann & Striessnig, 1990), may simply reflect stabilisation of higher affinity conformations of the DHP–receptor complex. This assumption is supported by the observation that binding stimulation by (+)-*cis*-diltiazem is more pronounced for DHPs with low B_{max} values (like for example [^{3}H]BAYK8644) than for those with higher binding densities (like for example (+)-[^{3}H]isradipine) (Glossmann et al., 1985).

Structural Implications. The higher relative quantum yield of specifically bound DMBODIPY-DHP suggests a conformational change of the DMBODIPY-DHP molecule upon association with its site. This increase clearly does not reflect an intrinsic property of the DMBODIPY fluorophore itself and is only observed after attachment to the DHP ring. It must therefore result from intramolecular quenching of DMBODIPY by the DHP moiety. In polar solvents intramolecular stacking is expected to occur between the hydrophobic rings of the fluorophore (DMBODIPY) and the substituted DHP ring. Less polar solvents will disrupt stacking interactions resulting in a conformational change leading to an increased average distance between the ring systems thereby decreasing intramolecular quenching. The elimination of intramolecular quenching upon drug binding therefore also suggests the formation of a more extended conformation of the DMBODIPY-DHP molecule in the bound state (Figure 1C). This is compatible with previous photoaffinity-labeling studies using nonfluorescent DMBODIPY-DHP analogues (azidopine and diazipine) that carry photoreactive substituents in the C-3 position (Catterall & Striessnig, 1992; Nakayama et al., 1991; Striessnig et al., 1991). Their photoreactive C-3 side chains interact with amino acid residues (close to transmembrane domain S6 in domain IV) remote from the site that binds the DHP ring (transmembrane domain IIIS6).

The FRET technique should be suitable for providing further information about the DHP binding domain. The efficiency of radiationless energy transfer is inversely correlated with the sixth power of the distance between two fluorophores (Lakowicz, 1983; Stryer & Haugland, 1967). Therefore one or more tryptophan residues located within or in close proximity to the DHP binding domain are probably involved in energy transfer. Inspection of the primary structure of the rabbit skeletal muscle Ca^{2+} channel α_1-subunit reveals that several tryptophan residues (Trp) are present in the proposed DHP binding regions next to the transmembrane S6 helices in domains III (Trp-1016) and IV (Trp-1391, Trp-1406) (Tanabe et al., 1987). Their contribution to energy transfer must be directly addressed by comparing the effect of substitution of these residues on transfer efficiency in mutated α_1-subunits.

Energy transfer efficiency also critically depends on the relative orientation of the dipoles of the participating fluorophores. Conformational changes of the α_1-subunit, induced by its interaction with drugs, toxins, or cations (for example, Ca^{2+}), may thus also be detectable with this technique. In our experiments (Figure 3B) the FRET signal in the absence and presence of noncompetitive modulators always correlated with the concentration of bound ligand, suggesting that drug-induced relative changes of fluorophore orientation are either absent or too small to be detected as a change of transfer efficiency under our experimental conditions.

We demonstrate that FRET between DHPs and Ca^{2+} channel α_1-subunits can be used to easily measure specific binding at very high time resolution. A simple step-wise reaction scheme was sufficient to calculate the full body of association and dissociation reactions with the same set of parameters. Furthermore, this step-wise binding mechanism explains the previously reported discrepancies between receptor densities reported for different ligands. High resolution binding assays should provide further insight into the molecular mechanisms of high affinity interaction of DHPs and other drugs with voltage-gated L-type Ca^{2+} channels.

ACKNOWLEDGMENT

We thank Dr. T. Brauns, E. Penz, and D. Reimer for providing partially purified Ca^{2+}-channel preparations and Dr. O. Wolfbeis (Institut für Organische Chemie, Universität Graz, Austria) and Dr. H. Gruber (Institut für Biophysik, Universität Linz) for helpful discussion.

REFERENCES

Bean, B. P. (1989) *Annu. Rev. Physiol. 51*, 367–384.

Bradford, M. M. (1976) *Anal. Biochem. 72*, 248–254.

Catterall, W. A., & Striessnig, J. (1992) *Trends Pharmacol. Sci. 13*, 256–262.

DeLean, A., Munson, P. J., & Rodbard, D. (1978) *Am. J. Physiol. 4*, E97–E102.

Glossmann, H & Ferry, D. R. (1985) *Methods Enzymol. 109*, 513–550.

Glossmann, H., & Striessnig, J. (1990) *Rev. Physiol. Biochem. Pharmacol. 114*, 1–105.

Glossmann, H., Ferry, D. R., Goll, A., Striessnig, J., & Zernig, G. (1985) *Drug Res. 35*, 1917–1935.

Knaus, H. G., Moshammer, T., Kang, H. C., Haugland, R. P., & Glossmann, H. (1992a) *J. Biol. Chem. 267*, 2179–2189.

Knaus, H. G., Striessnig, J., Hering, S., Marrer, S., Schwenner, E., Höltje, H.-D., & Glossmann, H. (1992b) *Mol. Pharmacol. 41*, 298–307.

Knaus, H. G., Moshammer, T., Friedrich, K., Kang, H. C., Haugland, R. P., & Glossmann, H. (1992c) *Proc. Natl. Acad. Sci. U.S.A. 89*, 3586–3590.

Lakowicz, J. R. (1983) *Principles of Fluorescence Spectroscopy*, Plenum Press, New York.

Nakayama, H., Taki, M., Striessnig, J., Glossmann, H., Catterall, W. A., & Kanaoka, Y. (1991) *Proc. Natl. Acad. Sci. U.S.A. 88*, 9203–9207.

Prinz, H., & Striessnig, J. (1993) *J. Biol. Chem. 268*, 18580–18585.

Schneider, T., Regulla, S., & Hofmann, F. (1991) *Eur. J. Biochem. 200*, 245–253.

Striessnig, J., & Glossmann, H. (1991) *Methods Neurosci. 4*, 210–229.

Striessnig, J., Moosburger, K., Goll, A., Ferry, D. R., & Glossmann, H. (1986) *Eur. J. Biochem. 161*, 603–609.

Striessnig, J., Murphy, B. J., & Catterall, W. A. (1991) *Proc. Natl. Acad. Sci. U.S.A. 88*, 10769–10773.

Striessnig, J., Berger, W., & Glossmann, H. (1993) *Cell. Physiol. Biochem. 3*, 295–317.

Stryer, L., & Haugland, R. P. (1967) *Proc. Natl. Acad. Sci. U.S.A. 58*, 719–726.

Tanabe, T., Takeshima, H., Mikami, A., Flockerzi, V., Takahashi, H., Kangawa, K., Kojima, M., Matsuo, H., Hirose, T., & Numa, S. (1987) *Nature 328*, 313–318.